

# Contact Pressure Distribution over MEA of a Three-Cell PEMFC with Metallic Bipolar Plates

K. Mohammadi<sup>1</sup>, M.M. Barzegari, M. Ghadimi, M. Momenifar

Northern Research Center for Science and Technology, Malek Ashtar University of Technology, Iran

## Article Information

Article History:

Received:

23 Nov 2022

Received in revised form:

12 Dec 2022

Accepted:

25 Dec 2022

## Keywords

PEMFC stack  
contact pressure distribution  
metallic bipolar plates  
pressure-sensitive film

## Abstract

One parameter that plays an important role in polymer electrolyte membrane fuel cells (PEMFCs) efficiency is the contact pressure between the bipolar plates and membrane electrode assembly (MEA). Increasing or decreasing the contact pressure between the plates causes ohmic losses and decreases the efficiency of the fuel cell. In this research, the contact pressure distribution over the MEA in a three-cell fuel cell stack with metallic bipolar plates with an active area of 100 cm<sup>2</sup> was investigated numerically and experimentally. Abaqus finite element software has been used for finite element simulation. Due to the asymmetry of the flow field of metallic bipolar plates, a full three-dimensional model was used for simulation. In addition, pressure-sensitive Fujifilm was used to experimentally investigate the contact pressure distribution on the MEA. Since the fuel cell stack includes three cells, the pressure-sensitive film was used in the middle cell, and thin insulating plates were used in the first and third cells. Finally, after disassembling the fuel cell stack and separating the pressure-sensitive film, the experimental test results were compared with the simulation results. The simulation results showed that the pressure changes on the active area were less than 0.3 MPa. The average contact pressure on the active area with a press force of 3.7 tons was about 1 MPa. Also, the results of the experimental tests were in good agreement with the simulation results.

## 1. Introduction

One of the most important influencing factors in the development of countries is the energy supply. The

reduction in fossil fuel resources and the pollution caused by the use of these fuels have prompted humans to research suitable alternatives for energy production. One of these, Fuel cell technology, can be used in transportation and power plants. Based on the

\*Corresponding Author: : kamal.mohammadi@mut.ac.ir

type of electrolyte, fuel cells can be classified into five categories: solid oxide, phosphoric acid, alkaline, molten carbonate, and PEMFCs.

PEMFCs have received more attention than other fuel cells due to their advantages, such as low operating temperature, high power density, and low start-up time. This type of fuel cell is made up of different components, including end plates, bipolar plates, current collector plates, sealants, and MEA. In a fuel cell, fuel is continuously injected into the anode electrode and oxygen into the cathode electrode. Electrochemical reactions are carried out in the electrodes, resulting in the creation of an electric current. This current reaches the bipolar plates by passing through the gas diffusion layer (GDL), and then it is transferred to the current collector plates and used.

Bipolar plates play an important role in volume, power density, water management, and, ultimately, power generation. In recent years, metallic bipolar plates have attracted much attention due to their excellent mechanical, electrical, and thermal properties, as well as their low cost and good manufacturability. In addition, metallic bipolar plates are thinner than graphite bipolar plates, which improves the power density of the fuel cell.

The contact pressure between the fuel cell plates plays an important role in the efficiency by causing ohmic losses in the fuel cell. The contact pressure between the bipolar plates and the MEA includes the most important part of the ohmic losses in the fuel cell. Since the amount of compressive stress between these two plates affects the amount of contact pressure, the increase of compressive stress between two plates and complete contact decreases the value of ohmic resistance. On the other hand, as the pressure increases, the amount of porosity in the GDL decreases and reduces the active surface, thus reducing the efficiency of the fuel cell. Therefore, the pressure applied from the bipolar plates to the GDL should be uniform and optimal over the entire surface. Furthermore, the amount of end plate deformation directly affects the pressure

distribution on the fuel cell plates. So, the lower the deformation of the end plates, the more uniform the contact stress distribution on the MEA.

Much research has been done on fuel cell efficiency as well as the effect of design and assembly parameters on PEM fuel cell performance. Chang et al. [1] investigated the effect of clamping force on fuel cell efficiency. They investigated the effect of compressive stress on porosity and electrical resistance. Lee et al. [2] studied the effect of GDL compression on fuel cell efficiency. Their results showed that an excessive increase in compressive force retains humidity and prevents its excretion. Also, the amount of porosity and contact resistance decreased with increasing pressure. Xiu et al. [3] worked on the optimization of the clamping force. They studied two goals, the first was to create a three-dimensional model, and the second was to investigate the effect of the clamping force on the GDL and its properties and fuel cell performance. Yim et al. [4] studied the effect of clamping force on fuel cell efficiency. In this research, the effect of GDL compression on 5-cell fuel cell efficiency has been studied experimentally. The GDL was tested in two conditions, with 15% compression and 30% compression. The results show that the efficiency increased with the increase in the amount of compression. Jibabin et al. [5] investigated the effect of GDL density on fuel cell performance. Jun Ni et al. [6] presented a mechanical-electrical model to predict the electrical resistance between bipolar plates and the GDL. Also, the effect of a chamfered radius in the channel walls of bipolar plates on electrical resistance was investigated.

However, limited research has been done on compressive stress and the improvement of contact pressure distribution on MEA. Lee et al. [7] investigated pressure distribution on the MEA and also studied the deformation rate of the end plate with the help of simulation. Karral and Me'le' [8] designed a finite element model and investigated the effect of the number of PEMFC cells on the pressure distribution of the

MEA. Alizadeh et al. [9] also investigated the effect of the end plate thickness and material, gasket hardness, and the number of PEMFC cells on the distribution of the contact stress applied to the MEA. They also investigated the contact pressure distribution on the active area of the PEMFC's MEA with a new clamping mechanism numerically and experimentally [10]. They concluded that the contact pressure distribution of MEA for the new clamping mechanism is more uniform than the conventional one. Barzegari et al. [11] investigated the effects of the geometrical parameters of an endplate with a curvature (bomb-shaped endplate) on the contact pressure distribution over the MEA. They manufactured and assembled a single fuel cell using simulation parameters and conducted experimental tests using pressure measurement film to evaluate the design. Liu et al. [12] studied the contact pressure distribution using a novel pneumatic clamping mechanism. Using this mechanism, they achieved better electrochemical performance for a PEMFC single cell. Peng et al. [13] presented an efficient approach to improve the contact pressure on the GDL by optimizing the amount of clamping force as well as the position of applying force on the end plates. They also investigated the effect of the number of PEMFC cells on the contact pressure distribution on the GDL of different cells of a PEMFC stack [14]. Lin et al. [15] discussed the influence of the cell number on the distribution characteristics of the contact pressure on the outermost and innermost GDLs in different stacks. They proposed a strategy to optimize the clamping condition of large-scale stacks based on calculating and predicting the contact pressure distribution on the GDLs in small-scale stacks.

The purpose of this research is to numerically and experimentally investigate the contact pressure distribution on the MEA in the three-cell stack of a fuel cell with metallic bipolar plates with an active area of 100 cm<sup>2</sup> and compare the results. In this research, a three-cell stack with metallic bipolar plates was assembled with the help of a torque meter, the contact pressure

distribution on the MEA was investigated using a pressure-sensitive film, and the test results were compared with the simulation results.

## 2. Three-cell PEM fuel cell stack

Fig. 1 shows the assembled three-cell stack with metallic bipolar plates. The stack includes two end plates, two current collectors, and four metallic bipolar plates, which are placed next to each other with the help of clamping rods.

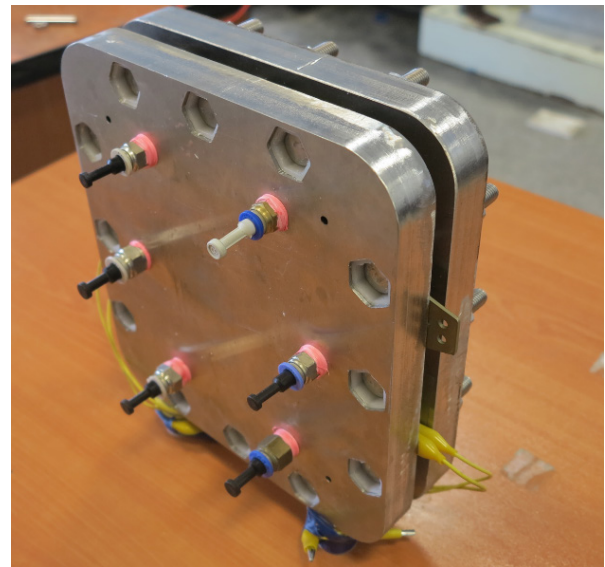


Fig. 1. The assembled three-cell stack with metallic bipolar plates.

### 2.1. Metallic bipolar plates

Among the various components of the fuel cell, the bipolar plates effectively contribute to determining the fuel cell's volume, weight, and cost. These plates account for 60% to 80% of the weight and volume and 15% to 45% of the total cost of a PEMFC.

Metallic bipolar plates have special advantages, and their material is selected based on the criteria of mechanical properties, formability, hydrogen permeabil-

ity, corrosion resistance and contact resistance, and price. However, due to their high price, noble metals such as gold and platinum, which have good corrosion resistance, have never reached commercialization. Other metals, such as aluminum and nickel, have good corrosion resistance by creating a superficial layer but are not a suitable option due to contact electrical conductivity weakness. Stainless steels are the only materials that have been considered for mass production. These materials are ideal for the production of bipolar plates, except in terms of corrosion and contact resistance. To be used in the fuel cell environment,

stainless steels must undergo a surface coating process to improve its corrosion resistance and contact resistance performance.

Among the methods for making metallic bipolar plates, forming processes are considered a suitable option in terms of high dimensional accuracy, good surface quality, high production rate, and low production cost. Stamping, hydroforming, rubber pad forming, gas forming, and electromagnetic forming are among the methods of forming metallic bipolar plates. The model of a metallic bipolar plate with an active area of 100 cm<sup>2</sup> is shown in Fig. 2.

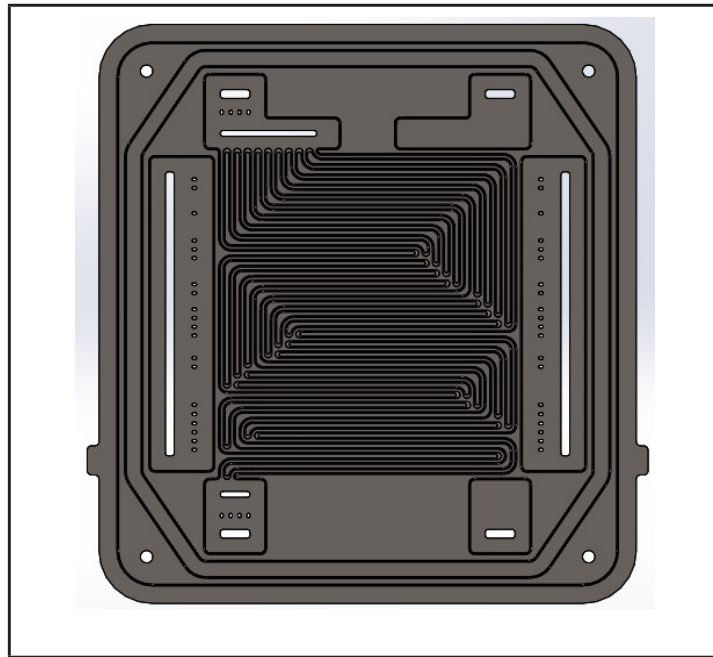


**Fig. 2.** The metallic bipolar plate model with an active area of 100 cm<sup>2</sup>.

The forming process of metallic bipolar plates in this study was done by the stamping method and with the help of two mold pieces, the die and punch. The design of the forming die is according to the model of metallic bipolar plates. The active area of the metallic bipolar plates is 100 cm<sup>2</sup>. Before the forming process,

the sheets are subjected to a cutting process (using a laser or wire cut machine) to create the required holes for the entry and exit of gases and water. An image of the metallic bipolar plates after the cutting and forming processes is shown in Fig. 3.

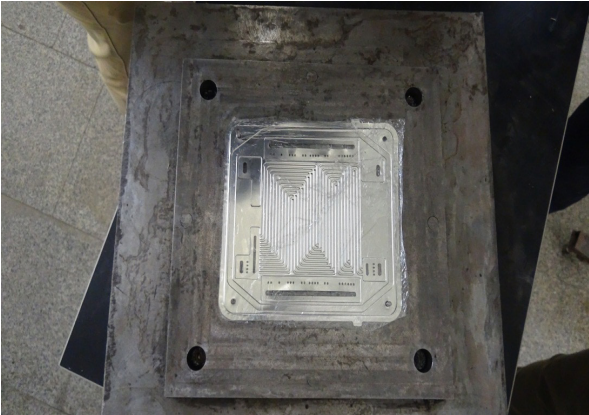


Fig. 3. The formed metallic bipolar plate after cutting and forming processes.

Next, the metallic bipolar plates are welded together to seal different locations between the two bipolar plate. Fig. 4 shows welded metallic bipolar plate.

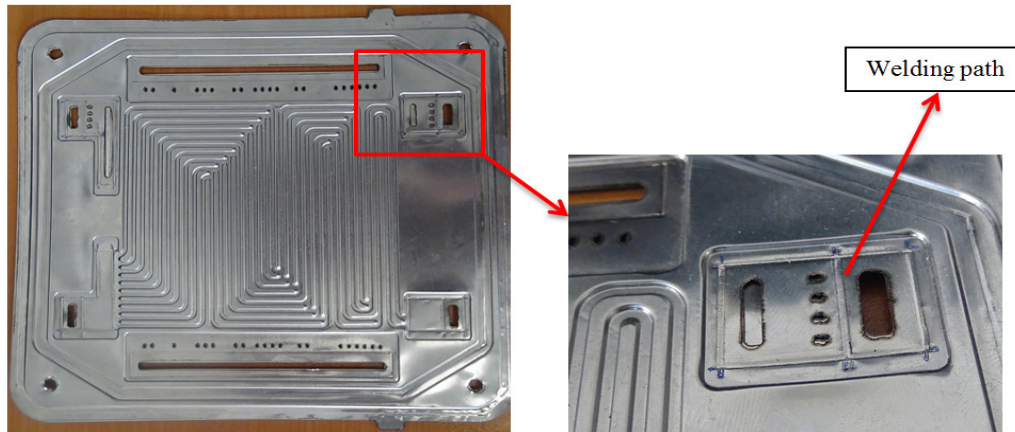


Fig. 4: The welded metallic bipolar plates.

After the welding process, the metallic bipolar plates are coated using the physical vapor deposition (PVD) method to reduce contact resistance. Three layers were coated on the metallic bipolar plates. A TiN coating with a thickness of  $1\ \mu\text{m}$  was chosen as the first layer to increase the coating adhesion to the steel substrate and to increase the corrosion resistance against sulfuric acid. A TiN- TiCN two-layer coating with a thickness of  $2\ \mu\text{m}$  was used in the second layer. Adding carbon increases wear resistance and also increases electrical conductivity. In the final layer, a TiN coating with a thickness of  $1\ \mu\text{m}$  was used to create abra-

sion resistance and also increase corrosion resistance against sulfuric acid.

## 2.2. Mechanical properties of PEM fuel cell components

Two 316L stainless steel formed sheets with a thickness of 0.1 mm were welded from the sides to a flat steel sheet with a thickness of 0.2 mm to produce the metallic bipolar plate. The thickness of a metallic bipolar plate after the welding process, including the depth of forming the sheets from both sides, reached 1.7 mm, which is thinner than the usual graphite bipo-

lar plates used in fuel cells. The mechanical properties of the components used in the simulation are listed in Table 1. In this paper, 60 Shore A Ethylene propylene diene monomer (EPDM), a kind of elastomer, was used as fuel cell sealant. Generally, an elastomer is assumed to be incompressible. Stress-strain data ob-

tained from the experimental results were used in Abaqus to define the hyperelastic properties of sealants and to find optimum strain energy density. The Neo-Hookean model agreed well with the uniaxial compression test data and was therefore used to simulate sealant properties [9].

**Table 1: Mechanical properties of components used in the fuel cell stack.**

component	material	Thickness (mm)	Module of elasticity (MPa)	Poisson's ratio	Density (Kg/m <sup>3</sup> )
GDL	Carbon paper	0.27	10	0.25	400
Bipolar	SS 316L	1.7	209000	0.3	7800
End plates	SS 316L	25	209000	0.3	7800
Current collectors	Coated SS 316L	2	209000	0.3	7800

### 3. Finite element simulation

In the current research, Abaqus versions 6.14 and 2020 were used to simulate the contact pressure distribution on the MEA. The purpose of the simulation is to investigate the contact pressure distribution in different areas of the MEA and compare it with the experimental results. In this simulation, the end plates are considered to be deformable of the solid type; the other components were considered deformable of the shell type. Eight-node linear brick reduced integra-

tion elements (C3D8R) were used to mesh the model's components. The dimensions of the sheet element were 0.1 mm, and the elements of the MEA and end plates were selected to be 0.5 mm. The contact properties were assumed to be a penalty with the contact surfaces, one of which is a sealant with the friction of 0.3 and the other 0.1. The meshed model of the assembly, including metallic bipolar plates, MEA, sealing lines, and end plates, is shown in Fig. 5. One-eighth of the PEMFC is modeled due to symmetric conditions with respect to all three Cartesian coordinate axes. The pressure applied on the end plate is equivalent to the load of the bolts.

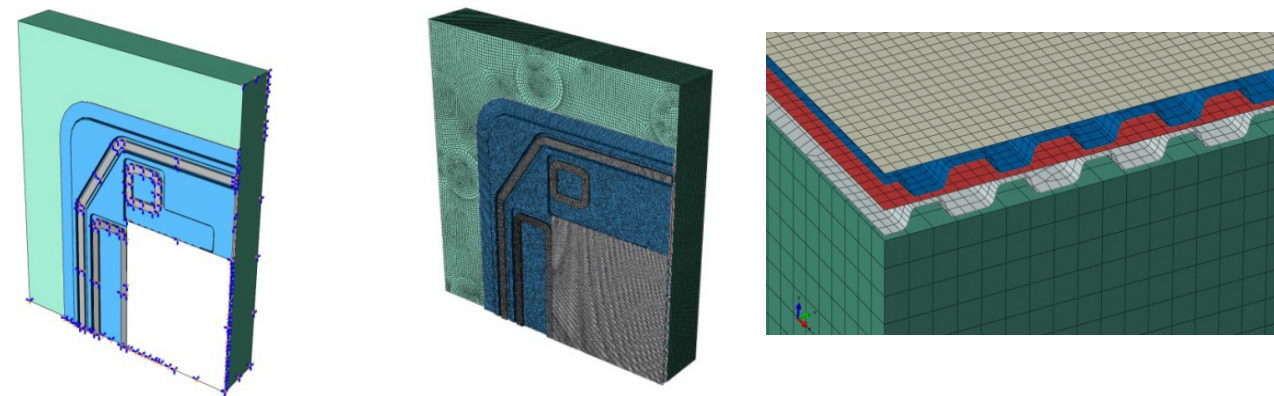


**Fig. 5. Finite element model.**

## 4. Experimental test

The Fujifilm pressure-sensitive film was used to investigate the contact pressure distribution on the MEA of a three-cell stack with metallic bipolar plates. Consid-

ering that the fuel cell stack includes three cells, the pressure-sensitive film is used in the middle cell, and thin insulating sheets are used in the first and third cells. The pressure-sensitive film replaces the membrane, and a GDL is used on both sides of the pressure-sensitive film. The assembly model of the three-cell stack can be seen in Fig. 6.

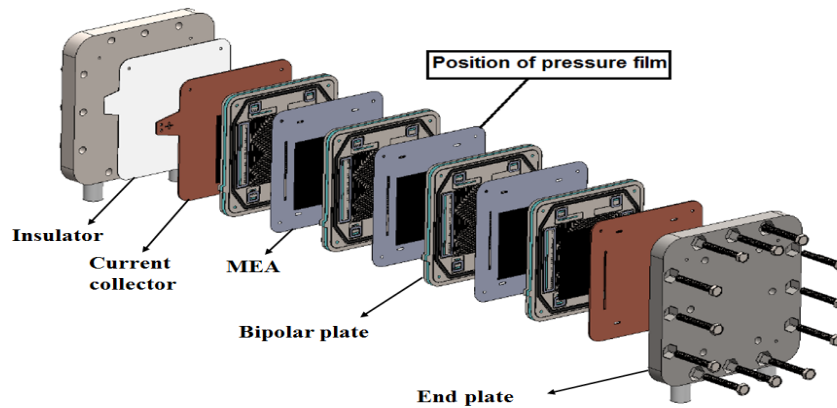


Fig. 6. Three-cell stack assembly model with metallic bipolar plates.

As can be seen in Fig. 6, the stack consists of metallic bipolar plates, MEA, current collector plates, and end plates put together under a certain pressure with the help of clamping rods.

As mentioned before, a pressure-sensitive film was used to investigate the contact pressure distribution on the MEA of the stack with metallic bipolar plates. The pressure-sensitive film contains microcapsules that burst and turn red when pressure is applied. Therefore, the achieved color density directly correlates with the amount of pressure applied on the

plates. The pressure-sensitive film is first cut according to the dimensions of the bipolar plates, and then guide pin holes are created on it to match the assembly exactly.

The assembly method of the pressure-sensitive film in the stack is shown in Fig. 7. As can be seen, a pressure-sensitive film is used in the middle cell, and thin insulating plates are used in the first and third cells in the three-cell stack. In fact, the pressure-sensitive film replaces the MEA, and a GDL is used on both sides of the film.

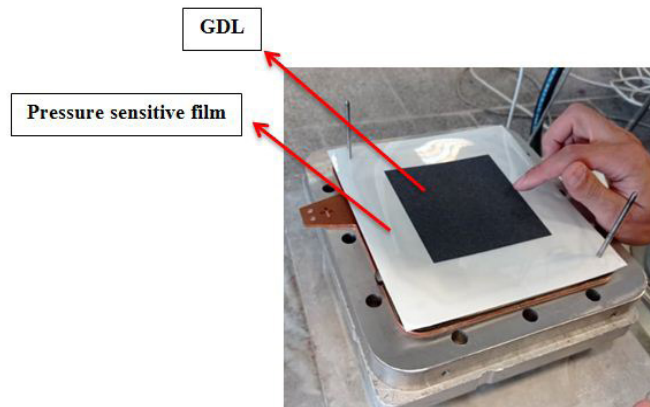


Fig. 7. The assembly of the pressure-sensitive film in the three-cell stack.

Of course, it should be noted that the bolts are tightened crosswise with the help of a torque meter to the desired torque. This research used an ACDelco digital torque meter with 50 N.m capacity, accuracy of  $\pm 2\%$ , and resolution of 0.1 N.m to distribute pressure uniformly during the assembly process. A few minutes after the complete assembly of the stack, the system can be disassembled, and the pressure-sensitive film can be removed. In this research, the temperature of the test place was measured at 25 °C, and the humidity of the place was measured at 50%, which should be considered in the analysis of contact pressure distribution over the MEA.

### 5. Results and discussion

The results of the simulation of contact pressure distribution on the MEA were obtained according to the loading and the considered boundary conditions of the assembly, see Fig. 8. As shown in Fig. 8, the contact pressure distribution in different areas is uniform and the average pressure applied on the MEA is around 1 MPa. The pressure distribution along the perpendicular bisector of one side of MEA is presented in a three-dimensional model to show the contact pressure distribution over the MEA, see Fig. 9. As shown in this figure, the amount of contact pressure along the mentioned axis is between 0.8 to 1.1 MPa.

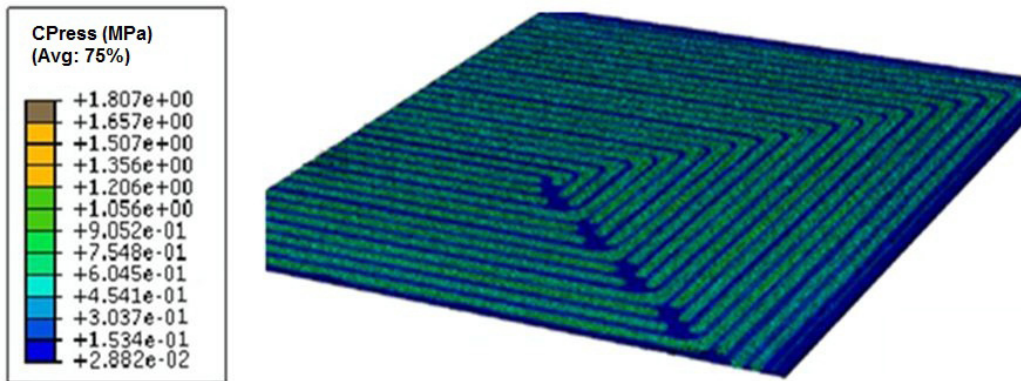


Fig. 8. Contact pressure distribution over the MEA.

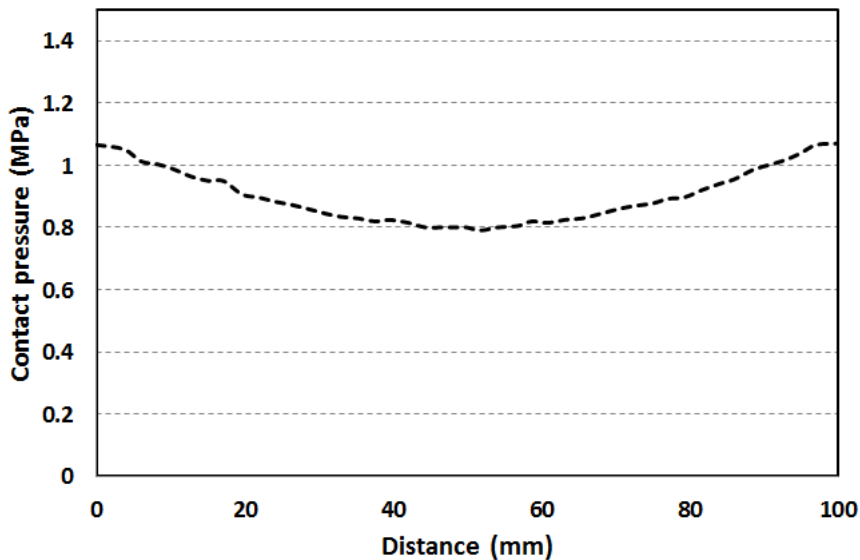
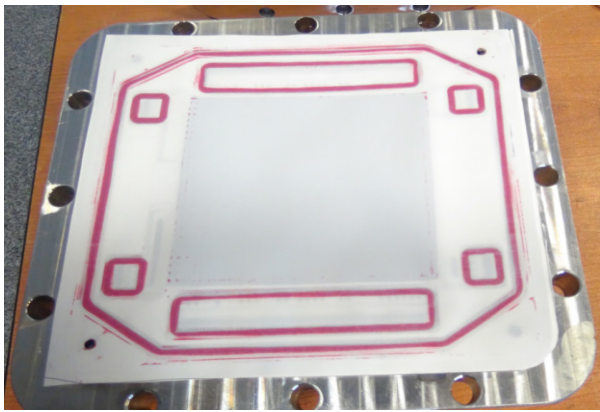
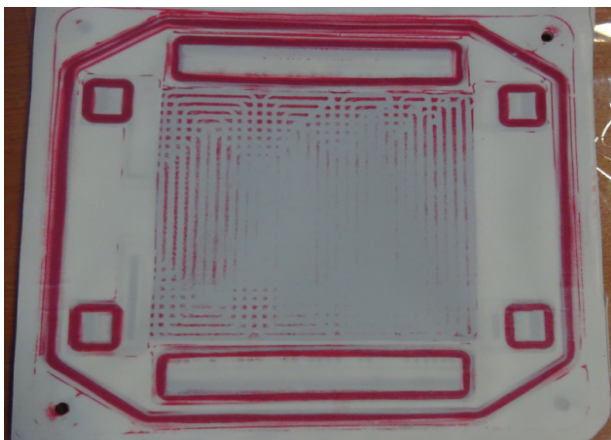


Fig. 9. Contact pressure distribution over the MEA along the x axis

In order to perform the experimental tests, the three-cell stack was first assembled with the help of a torque meter under torques of 7 and 10 N.m, which did not lead to a favorable result in terms of pressure distribution. Fig. 10(a) shows the pressure-sensitive film removed from the stack, where the stack is assembled under a torque of 7 N.m with the help of a torque meter. As can be seen from the figure, only the effect of the sealing lines on the film is visible due to the low pressure, and there is no gas flow field effect on the film. However, by increasing the torque of the bolts to 10 N.m, in addition to the sealing lines' effect, some of the flow field's effects can also be seen on the film, as shown in Fig. 10(b).



(a)



(b)

Fig. 10. Pressure distribution of the stack, (a) with torques of 7 N.m and (b) with torques of 10 N.m.

Finally, by increasing the torque of the stack bolts to 13 N.m, the pressure distribution on the MEA is uniform, see Fig. 11.

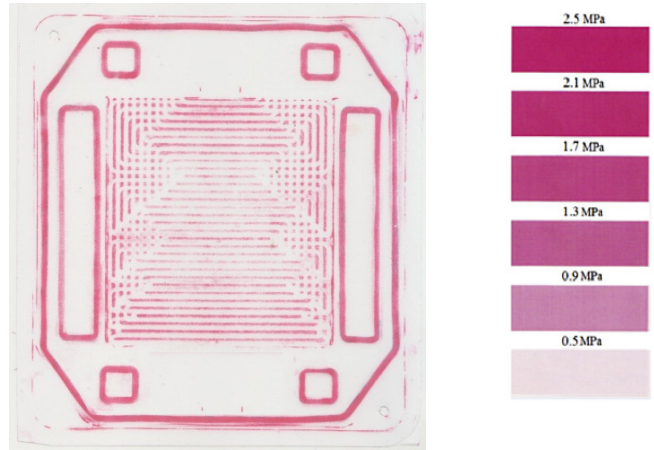


Fig. 11: Contact pressure distribution at a torque of 13 N.m.

In addition, the contact pressure distribution over the MEA surface was investigated by applying the clamping force using a press machine. Fig. 12 shows the pressure-sensitive film result on the MEA with 3.7 tons of clamping force applied on the stack.

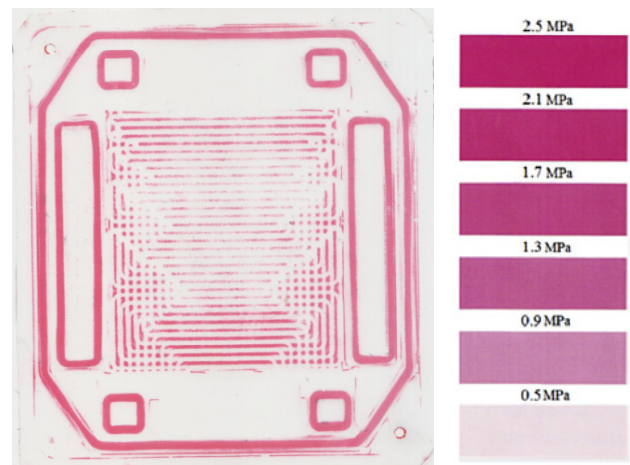


Fig. 12. The result of the pressure distribution test on the stack with the press machine.

It should be noted that a special scanner was used to measure the quantitative values of pressure applied to the MEA. First, the pressure-sensitive film obtained from the experimental test was scanned with the help

of this scanner. Then, the numerical value of the pressure was determined by analyzing the obtained color density and comparing it with the catalogs provided by the pressure-sensitive film manufacturer.

---

## 6. Conclusion

In this research, the contact pressure distribution on the MEA was investigated in a three-cell stack with metallic bipolar plates and an active area of 100 cm<sup>2</sup>. First, the three-dimensional model of the PEMFC was prepared in Abaqus software. It was assumed that the symmetry constraint with respect to the Cartesian coordinate axes was one-eighth of the PEMFC. Then, in order to validate the simulation results, a three-cell stack with metallic bipolar plates was assembled, and pressure-sensitive films were used to measure the contact pressure distribution experimentally. A torque meter and a press machine applied the clamping force on the stack. The results reveal that the contact pressure distribution over the MEA surface is uniform in both numerical and experimental states, and they are in good agreement with each other. The simulation results showed that the pressure changes on the active area are less than 0.3 MPa. The average pressure value in these two states is almost equal and is around 1 MPa. In addition, to determine the amount of applied force on the bolts in the simulation, the equivalent pressure of each bolt torque was applied using a press machine. Furthermore, the results reveal that the selected thickness of the end plates is suitable and has adequate flexural rigidity to overcome the end plates' deflection due to the applied torque on the bolts.

## References

- [1] W.R. Chang, J.J. Hwang, F.B. Weng, S.H. Chan, 2007. "Effect of clamping pressure on the performance of a PEM fuel cell", *Journal of Power Sources*, 166, 149–154.
- [2] Woo-kum Lee, Chien-Hsien Ho, J.W. Van Zee, Mahesh Murthy, 1999. "The effects of compression and GDLs on the performance of a PEM fuel cell", *Journal of Power Sources*, 84, 45–51.
- [3] Xiu Qing Xing, KahWai Lum, Hee Joo Poh, Yan LingWu. 2010. "Optimization of assembly clamping pressure on performance of proton-exchange membrane fuel cells". *Journal of Power Sources*, 195, 62–68.
- [4] Sung-Dae Yim, Byung-Ju Kim, Young-Jun Sohn, Young-Gi Yoon, Gu-Gon Park, Won-Yong Lee, Chang-Soo Kim, Yong Chai Kim. 2010. "The influence of stack clamping pressure on the performance of PEM fuel cell stack". *Current Applied Physics*, 10, S59–S61.
- [5] Jiabin Ge, Andrew Higier, Hongtan Liu. 2006. "Effect of GDL compression on PEM fuel cell performance". *Journal of Power Sources*, 159, 922–927.
- [6] Xinmin Lai, Dong'an Liua, Linfa Penga, Jun Ni. 2008. "A mechanical–electrical finite element method model for predicting contact resistance between bipolar plate and GDL in PEM fuel cells". *Journal of Power Sources*, 182, 153–159.
- [7] Shuo-Jen Lee, Chen-De Hsu, Ching-Han Huang. 2005. "Analyses of the fuel cell stack assembly pressure". *Journal of Power Sources*, 145, 353–361.
- [8] Christophe Carral, Patrice Me'le'. 2014. "A nu-

- merical analysis of PEMFC stack assembly through a 3D finite element model“. *International journal of hydrogen energy*, 39, 4516 e4530.
- [9] Alizadeh E, Barzegari MM, Momenifar M, Ghadimi M, Saadat SHM, 2016. "Investigation of contact pressure distribution over the active area of PEM fuel cell stack“, *International Journal of Hydrogen Energy*, 41, 3062-71.
- [10] Alizadeh, E., Ghadimi, M., Barzegari, M. M., Momenifar, M., & Saadat, S. H. M. 2017. Development of contact pressure distribution of PEM fuel cell's MEA using novel clamping mechanism. *Energy*, 131, 92-97.
- [11] Barzegari, M. M., Ghadimi, M., Habibnia, M., Momenifar, M., & Mohammadi, K. 2020. Developed endplate geometry for uniform contact pressure distribution over PEMFC active area. *Iranian Journal of Hydrogen & Fuel Cell*, 7(1), 1-12.
- [12] Liu, J., Tan, J., Yang, W., Li, Y., & Wang, C. 2021. Better electrochemical performance of PEMFC under a novel pneumatic clamping mechanism. *Energy*, 229, 120796.
- [13] Yongbo Qiu, Peng Wu, Tianwei Miao, Jinqiao Liang, Kui Jiao, Tao Li, Jiewei Lin, Junhong Zhang, 2020 . "An Intelligent Approach for contact pressure optimization of PEM fuel cell GDLs“, *applied sciences*, 10, 4194.
- [14] Jiewei Lin, Peng Wu, Huwei Dai, Yongbo Qiu, Junhong Zhang, 2020 . "Intelligent optimization of clamping design of PEM fuel cell stack for high consistency and uniformity of contact pressure“, *contact pressure International Journal of Green Energy*, 10, 1080.
- [15] Lin, J., Wu, P., Dai, H., Qiu, Y., & Zhang, J. 2022. Intelligent optimization of clamping design of PEM fuel cell stack for high consistency and uniformity of contact pressure. *International Journal of Green Energy*, 19(1), 95-108.